Climatic Change (2007) 84:337–363
DOI 10.1007/s10584-007-9256-1

# A comparison of explicit and implicit spatial downscaling of GCM output for soil erosion and crop production assessments

**X-C Zhang**

Received: 26 January 2006 / Accepted: 13 March 2007 / Published online: 27 April 2007


**Abstract** Spatial downscaling of climate change scenarios can be a significant source of uncertainty in simulating climatic impacts on soil erosion, hydrology, and crop production. The objective of this study is to compare responses of simulated soil erosion, surface hydrology, and wheat and maize yields to two (implicit and explicit) spatial downscaling methods used to downscale the A2a, B2a, and GGa1 climate change scenarios projected by the Hadley Centre's global climate model (HadCM3). The explicit method, in contrast to the implicit method, explicitly considers spatial differences of climate scenarios and variability during downscaling. Monthly projections of precipitation and temperature during 1950–2039 were used in the implicit and explicit spatial downscaling. A stochastic weather generator (CLIGEN) was then used to disaggregate monthly values to daily weather series following the spatial downscaling. The Water Erosion Prediction Project (WEPP) model was run for a wheat–wheat–maize rotation under conventional tillage at the 8.7 and 17.6% slopes in southern Loess Plateau of China. Both explicit and implicit methods projected general increases in annual precipitation and temperature during 2010–2039 at the Changwu station. However, relative climate changes downscaled by the explicit method, as compared to the implicit method, appeared more dynamic or variable. Consequently, the responses to climate change, simulated with the explicit method, seemed more dynamic and sensitive. For a 1% increase in precipitation, percent increases in average annual runoff (soil loss) were 3–6 (4–10) times greater with the explicit method than those with the implicit method. Differences in grain yield were also found between the two methods. These contrasting results between the two methods indicate that spatial downscaling of climate change scenarios can be a significant source of uncertainty, and further underscore the importance of proper spatial treatments of climate change scenarios, and especially climate variability, prior to impact simulation. The implicit method, which applies aggregated climate changes at the GCM grid scale directly to a target station, is more appropriate for simulating a first-order regional response of nature resources to climate change. But for the site-specific impact assessments, especially for entities that are heavily influenced by local conditions such as soil loss and crop yield, the explicit method must be used.

X.-C. Zhang (✉)
USDA-ARS Grazinglands Research Laboratory, 7207 West Cheyenne St., El Reno, OK 73036, USA
e-mail: jzhang@grl.ars.usda.gov

## 1 Introduction

The Intergovernmental Panel on Climate Change (IPCC (Intergovernmental Panel on Climate Change) 2001) has concluded that precipitation very likely increased by 0.5 to 1% per decade in the twentieth century over most mid- and high latitude land areas of the Northern Hemisphere, and the frequency of heavy precipitation events likely increased by 2–4% over the second half of the century as well. Across the contiguous United States, precipitation has increased by some 10% since 1910, and the increase has been primarily in the form of heavy and extreme daily storms (Karl and Knight 1998). Specifically, about 53% of the total national increase is due to the precipitation increase within the upper 10% of all the daily precipitation amounts since 1910. Groisman (see SWCS 2003) analyzed the trends in share of total annual precipitation occurring in heavy (>95th percentile), very heavy (>99th), and extreme daily precipitation events (>99.9th) in the contiguous U.S. between 1910–1970 and 1970–1999, and reported that the linear trends between the two periods increased by 4.6, 7.2, and 14.1% per decade, respectively, which are in contrast to the 1.2% increase per decade for total annual precipitation. Zhai et al. (1999) analyzed daily rainfall records across the contiguous China and reported that frequency of heavy storms, on average, decreased from 1951 to 1990, but intensity of heavy storms (mm $d^{-1}$) increased significantly. This bias toward more intense rainfall events is of great concern for assessing the potential impacts on soil erosion and surface hydrology because severe soil erosion and catastrophic environmental destruction are often caused by infrequent heavy storms.

Besides the historical trends, most Global Climate Models (GCMs) have projected that globally averaged mean water vapor, evaporation, and precipitation will be very likely to increase in the twenty-first century, and intensity of daily precipitation events will also likely to increase (IPCC (Intergovernmental Panel on Climate Change) 2001; U.S. NAST 2001). Most GCMs have also projected that increases in extreme precipitation and temperature in a warmer climate are likely to be much greater than increases in their means (Hegerl et al. 2004; SWCS 2003). An expert panel assembled by the Soil and Water Conservation Society after a thorough synthesis and review of historical climate trends as well as future GCMs projections has concluded that the potential for climate change to increase the risk of soil erosion, surface runoff, and related environmental consequences is clear (SWCS 2003). The panel further called for comprehensive and detailed evaluations of the potential impacts of climate change across various physiographical conditions at multiple temporal scales to answer two basic questions: whether a change in soil and water management practices is warranted under climate change and what adaptive measures should be taken if a change is warranted.

Physically based crop and erosion models, which are best suited to assess the impacts of climate change on soil erosion and crop production, require daily climate data at specific locations. Although some GCMs are capable of producing daily values at their grid scales, spatial downscaling is still needed to generate climate input to simulation models for a specific location of interest. If GCM-monthly projections are to be used, both spatial and temporal downscaling are required. Many methods have been developed to statistically downscale regional climate models (RCMs) or GCMs projections, among which stochastic weather generators are widely used (e.g., Wilks 1992; Semenov and Barrow 1997; Katz 1996; Mearns et al. 1997; Mavromatis and Jones 1998; Hansen and Ines 2005). A common approach in using weather generators is to adjust the ‘present-day’ climate parameters according to GCM-projected relative climate changes, and then to generate ‘future climate’ using perturbed parameter values. Both implicit and explicit spatial downscaling methods are employed in this approach. In the implicit method, relative climate changes such as precipitation ratios and

temperature shifts computed from climate projections at a GCM- or RCM-native grid box are used to directly adjust baseline daily time series established for a station (also referred as 'change factor' method), or to modify relevant climate parameters derived from the baseline climatology for stochastic generation of future climate (e.g., Favis-Mortlock and Savabi 1996; Mavromatis and Jones 1998; Pruski and Nearing 2002; Mearns et al. 2003; Hansen and Ines 2005; Zhang et al. 2004; O'Neal et al. 2005; Smith et al. 2005). This method does incorporate the climatic characteristics of the target station as well as the areal-averaged relative climate changes projected at the GCM grid level, but fails to consider differences between climate variability at the GCM grid scale and that at the target station. In the explicit spatial downscaling method, GCMs or RCMs projections at the native grid box are first downscaled to the target station using transfer functions, and stochastic weather generators are then used to generate daily weather series using climate parameters modified by the spatially downscaled climate scenarios or relative changes at the station scale (e.g., Wilby 1997; Semenov and Barrow 1997; Wilby et al. 1998; Kilsby et al. 1998; Diaz-Nieto and Wilby 2005; Zhang 2005).

Different downscaling methods often lead to statistically different realizations of daily weather series and therefore result in different soil erosion and runoff predictions for a given climate change scenario. For example, a simple proportional adjustment method (change factor), which directly scales up or down historical or generated daily precipitation series by GCM- or RCM-projected percent changes disregarding changes in number of wet days (e.g., Favis-Mortlock and Savabi 1996; Mearns et al. 2003; Wood et al. 2004), tended to overestimate simulated soil loss (Yu 2005). The overestimation of soil loss is attributed to the fact that when daily precipitation amount is scaled or multiplied by a ratio the variance of daily precipitation is multiplied by the square of the ratio. More importantly, how to handle projected climate variability (e.g., variance of daily and monthly precipitation) during downscaling is extremely important to soil erosion, runoff, and crop predictions. An increase in precipitation variance is accompanied by an increase in occurrence of heavy storms, which often have high intensity and therefore result in severe soil erosion (Zhang et al. 2004; Zhang and Nearing 2005). Nearing et al. (2005) have shown that soil erosion was quite sensitive to changes in total rainfall amounts associated with changes in either storm intensity or duration, and soil erosion was more sensitive to those changes than runoff. To date most soil erosion trends under climate change reported in literature are from model simulations without an explicit spatial downscaling of GCMs projections (Zhang 2005). This type of approach tends to provide a first order sensitivity of regional response to climate change (Hewitson 2003; Zhang and Liu 2005; Zhang 2006).

The Water Erosion Prediction Project (WEPP) model is a continuous daily simulation model (Flanagan and Nearing 1995). It contains erosion, hydrology, daily water balance, plant growth, and residue decomposition components, and uses a stochastic weather generator (CLIGEN) to generate daily weather data. The plant growth and water balance components are modified to account for the $CO_2$ effects on evapotranspiration (ET) and biomass production as described by Favis-Mortlock and Savabi (1996). The modified $CO_2$-sensitive version has been used to study the impacts of climate change on runoff and erosion (e.g., Savabi et al. 1993; Favis-Mortlock and Savabi 1996; Pruski and Nearing 2002; Zhang et al. 2004; O'Neal et al. 2005). Most studies showed that under similar crop management a 1% increase in annual precipitation would result in a 0.5–4% increase in annual soil loss and a 1–4% increase in surface runoff.

Climate change scenarios used in this study are from the recent climate change experiments conducted using a third generation general circulation model (HadCM3) at the Hadley Centre, UK (Gordon et al. 2000; Pope et al. 2000). The climate change scenarios

projected using the greenhouse gas emissions scenarios of A2, B2, and GGa are selected to represent relatively high, low, and intermediate $CO_2$ increases, respectively. Each scenario describes a possible demographic, economic, societal, and technological future. Since this is a methodology study, only one GCM and three emissions scenarios are used.

The Loess Plateau, which occupies 380,000 $km^2$ (Chen et al. 1988), is situated in the middle reaches of the Yellow River. It is covered with thick and highly erodible aeolian deposits. The climate varies from semiarid to subhumid, with heavy storms mostly falling in July through September. It is one of the most eroded regions in the world because of highly erodible soils, steep slopes, heavy storms, and low vegetation cover stemming from intensive cultivation and improper land uses. On average, suspended sediment of some 1.53 billion tons (equivalent to 5–6 mm soil depth) is delivered from the Loess Plateau each year, and about a quarter is deposited on the riverbeds in the lower reaches of the Yellow River, which are 3–12 m above the ground outside the stream banks and are rising at 8–10 cm each year (Chen et al. 1988). The wellbeing and safety of densely populated people in the lower reaches region are of great concern for the country. Undoubtedly, any increase in soil erosion and floods under climate change from the Loess Plateau would exacerbate the existing problems. Thus, a detailed assessment of climatic impact on soil erosion and water resources is warranted for the region, and is needed for developing national strategic mitigation plans.

The objective of this study is to compare responses of simulated soil erosion, surface hydrology, and crop production to two (implicit and explicit) spatial downscaling methods using the CLIGEN and WEPP models under three climate change scenarios of HadCM3 in the Loess Plateau of China. The monthly precipitation and maximum and minimum temperatures of the 2010–2039 period are temporally downscaled to daily time series with or without an explicit spatial downscaling for input to the WEPP model. The two downscaling methods form the basis of comparison in this study.

## 2 Materials and methods

### 2.1 Site description

The study site is located at the Changwu experiment station (35.2° N and 107.8° E) in the Loess Plateau region of China. The elevation is about 1,206.5 m above sea level. The prevailing landform is loessial tableland. The loess is more than 100-m thick on the tableland. The soils are predominantly silt loam with silt content greater than 50%. The average annual precipitation is 578 mm, with 55% falling in July through September. The annual average temperature is 9.2°C. The common regional cropping system is a three-year rotation of winter wheat–winter wheat–summer maize.

### 2.2 Wepp calibration

Measured soil properties, climate, crop management, surface runoff, and sediment yield from field runoff plots (20 m long by 5 m wide) from 1988 to 1992 were used to calibrate soil erodibility parameters of the WEPP model (v2004.7). Measured properties of the Huangmian soil series included soil texture, organic matter content, bulk density, hydraulic conductivity, wilting point water content, and field capacity of the soil profile (Table 1). Daily precipitation amount, rainfall duration, rainfall intensity, maximum and minimum temperature were measured. Two field runoff plots and two cropping systems were selected. One runoff plot (8.7% slope) was under

**Table 1** Soil properties used in the WEPP calibration and simulation

| Depth (cm) | Sand (%) | Clay (%) | Organic matter (%) | Bulk density (t $m^{-3}$) | Ks[a] (mm $h^{-1}$) | Field capacity ($m^3$ $m^{-3}$) | Wilting point ($m^3$ $m^{-3}$) | CEC[b] ($cmol_c$ $kg^{-1}$) |
|---|---|---|---|---|---|---|---|---|
| 0–20 | 8.0 | 34.8 | 0.75 | 1.41 | 3.7 | 0.305 | 0.094 | 7.5 |
| 20–40 | 7.5 | 34.8 | 0.53 | 1.41 | 4.6 | 0.305 | 0.094 | 6.0 |
| 40–60 | 7.3 | 34.8 | 0.53 | 1.38 | 6.3 | 0.313 | 0.115 | 6.0 |
| 60–80 | 7.2 | 32.9 | 0.41 | 1.31 | 6.7 | 0.311 | 0.110 | 5.8 |
| 80–100 | 8.0 | 33.3 | 0.41 | 1.26 | 6.8 | 0.309 | 0.106 | 5.8 |
| 100–180 | 9.5 | 36.8 | 0.54 | 1.40 | 6.8 | 0.309 | 0.106 | 5.8 |

[a] Saturated hydraulic conductivity; [b] Cation exchange capacity

conventionally tilled continuous bare fallow. Another plot (17.6% slope) was under conventionally tilled continuous soybean with residue removed after harvest. Soil erodibility was calibrated to the soil of both plots under the condition that measured average annual runoff matched WEPP-predicted runoff. Calibrated critical shear stress, interrill and rill erodibility for the soil were 3.5 Pa, $1.5\times10^6$ kg s $m^{-4}$, and 0.0025 s $m^{-1}$, respectively. The measured and calibrated average annual soil losses were 7.2 and 7.6 ton $ha^{-1}$, respectively, for continuous soybean, and 9.4 and 9.2 ton $ha^{-1}$ for continuous fallow.

Plant growth parameters for maize were taken directly from the WEPP technical documentation (Flanagan and Nearing 1995) with a biomass-energy conversion ratio of 28 kg $MJ^{-1}$ to represent the medium fertility level. For winter wheat, the calibrated parameter values were 0.5 for harvest index, 1,600 degree days (°C·day) for growing degree day to maturity, 35 kg $MJ^{-1}$ (high fertility) for biomass-energy conversion ratio, and 1.8 m for rooting depth. The rest of parameter values were taken from Flanagan and Nearing (1995). With the calibrated parameter values, simulated average annual grain yields under the present climate were 3.15 ton $ha^{-1}$ for wheat and 6.84 ton $ha^{-1}$ for maize, which agreed well with the regional average yields of 3.16 ton $ha^{-1}$ for wheat and 6.44 ton $ha^{-1}$ for maize between 1986 and 1999 (surveyed and compiled by the Changwu experiment station).

### 2.3 Stochastic climate generator (CLIGEN)

The CLIGEN model is a stochastic daily weather generator (Nicks and Gander 1994). It generates the occurrence of daily precipitation (related to precipitation frequency) using a first-order, two-state Markov chain based on transition probabilities of a wet day following a wet day ($P_{w/w}$) and a wet day following a dry day ($P_{w/d}$). The daily mean precipitation ($R_d$, mm) is generated using a transformed (skewed) normal distribution. The daily maximum and minimum temperatures are generated using normal distributions. In this study, means and variances of daily precipitation depths and temperatures as well as the two transition probabilities are modified to generate changed climates. Other parameters including skew coefficient of daily precipitation, storm characteristics such as storm duration, dew temperature, solar radiation, and wind speed and direction, which are generated in CLIGEN, are not adjusted. In CLIGEN, daily weather is generated on a monthly basis (i.e., no dependency between months), and each variable is generated independent of other variables. Because each variable is generated independently and for each month, incorporation of GCM-projected monthly changes either with or without an explicit spatial downscaling into model parameters is straightforward.

## 2.4 Explicit method

### *2.4.1 Spatial downscaling*

Spatial downscaling in this study is to downscale monthly precipitation and temperature of GCMs projections at a GCM grid box to monthly values at a specific location using transfer functions. Monthly precipitation and temperatures of 1957–2001 projected at the GCM grid box were used as control to develop transfer functions in conjunction with the baseline monthly data of the same period measured at the Changwu station for each calendar month. Monthly data of 2010–2039 projected at the grid box were then spatially downscaled to the Changwu station using the derived transfer functions.

The observed and GCM-projected monthly precipitation of 1957–2001 were analyzed for each calendar month. The ranked observational monthly precipitation (*Y*-axis) was plotted with the ranked GCM-projected precipitation (i.e., paired by their ranks or corresponding quartiles, also called qq-plot). A univariate linear and a nonlinear function were fitted to each plot to obtain transfer functions for each month using the LAB-fit software (Universidade Federal de Campina Grande, Brazil). This curve fitting software automatically searches through about 200 nonlinear functions having one independent variable and up to four fitting parameters, and returns a list of functions ranked by their residual errors.

Those transfer functions were then used to downscale 2010–2039 monthly precipitation at the native GCM scale to those at the Changwu station assuming that those transfer functions are applicable to the changed climate. Since the transfer functions are based on the distributions of monthly precipitation of 1957–2001, this assumption is deemed valid so long as future monthly precipitation of 2010–2039 falls in the ranges within which the transfer functions are established. However, the validity is questioned if future projections are outside the ranges. For better results, this method is more appropriately used with longer baseline records and for 'nearer-future' projections (say, next 20–30 years). For each calendar month, the nonlinear function was used to transform the projected monthly precipitation values that were within the range in which the nonlinear function was fitted, while the linear function was used for the values outside the range. The downscaled monthly precipitation values, which represent the future monthly precipitation distribution at the Changwu station, were used to calculate monthly mean and variance of the changed climate for the location for each month. Those means and variances of the downscaled monthly precipitation were used to estimate means and variances of daily precipitation, which are input parameters to CLIGEN for generating daily weather series of the changed climate for the Changwu station.

Likewise, the GCM-projected monthly maximum and minimum temperatures were downscaled spatially in the same manner as was for monthly precipitation. Mean temperature shifts as well as variance ratios between the downscaled monthly GCM projections of 2010–2039 and the local monthly measurements of 1957–2001 were calculated for each month.

### *2.4.2 Temporal downscaling*

Measured daily weather data of 1957–2001 at Changwu were used to estimate the baseline CLIGEN input parameters, which were subsequently adjusted to generate daily weather series of the changed climates for the station. For precipitation, adjusted precipitation parameters include mean ($R_d$) and variance ($\sigma_d^2$) of daily precipitation depths (excluding zeros) and conditional transition probabilities of a wet day following a dry day ($P_{w/d}$) and a

wet day following a wet day ($P_{w/w}$). For transition probability adjustment, linear relationships between transition probabilities and mean monthly precipitation ($R_m$) were developed for each calendar month using historical station records. For each calendar month (say January), some 25 wettest and driest months were selected to compute $P_{w/w}$, $P_{w/d}$, and $R_m$ for each group (note that some average years were used in both groups for longer records). Linear relationships between $P_{w/w}$ and $R_m$ as well as between $P_{w/d}$ and $R_m$ were established between the dry and wet groups. The adjusted $P_{w/w}$ and $P_{w/d}$ for the changed climate were linearly interpolated for the downscaled $R_m$ using the relationships. For convenience, the adjusted conditional transition probabilities are equivalently expressed in term of an unconditional probability of daily precipitation occurrence ($\pi$) and a dependence parameter ($r$) defined as the lag-1 autocorrelation of daily precipitation series:

$$\pi = \frac{P_{w/d}}{1 + P_{w/d} - P_{w/w}} \tag{1}$$

$$r = P_{w/w} - P_{w/d} \tag{2}$$

The adjusted mean daily precipitation per wet day ($R_d$) was estimated as:

$$R_d = \frac{R_m}{N_d \pi} \tag{3}$$

where $N_d$ is the number of days in the month and $N_d\pi$ is the average number of wet days in the month. New daily precipitation variance ($\sigma_d^2$) related to monthly precipitation variance at the station in the form of (Wilks 1999):

$$\sigma_d^2 = \frac{\sigma_m^2}{N_d \pi} - \frac{(1-\pi)(1+r)}{1-r} R_d^2 \tag{4}$$

For maximum and minimum temperature, downscaled monthly temperature means and temperature variance ratios between spatially downscaled monthly values of 2010–2039 and measured monthly values of 1957–2001 were calculated for each calendar month. Downscaled mean maximum and minimum temperatures were directly used in CLIGEN as the adjusted monthly means for the changed climate. Adjusted daily temperature variances were obtained by multiplying the baseline daily temperature variances by the aforementioned monthly variance ratios for each month. Parameter adjustment was made separately for each climate change scenario. All adjusted parameter values were input to CLIGEN (v5.111), and 100 years of daily weather data were generated for each climate change scenario.

### 2.5 Implicit method

This method is similar to the explicit method but without the spatial downscaling step. The monthly precipitation projected for the native grid box (containing the target station) for the periods of 1950–1999 and 2010–2039 was used to calculate mean precipitation ratios as well as variance ratios between the two periods for each month. Projected mean monthly minimum and maximum temperatures for the two periods were used to compute mean temperature shifts and variance ratios for both maximum and minimum temperatures for each month. Those relative changes calculated at the native grid box were directly applied

to the baseline climate parameters derived using observed daily data of Changwu without an explicit spatial downscaling.

For each month, new monthly mean precipitation at Changwu ($R_m$) was calculated by multiplying the observed baseline monthly precipitation mean by the mean ratio of GCM-projected monthly precipitation between 2010–2039 and 1950–1999. New $P_{w/w}$ and $P_{w/d}$ were interpolated for the new monthly mean precipitation using the established linear relationships presented in Section 2.4.2. New mean daily precipitation per wet day ($R_d$) was calculated using Eq. 3. New variance of daily precipitation under climate change was approximated by multiplying the baseline variance derived from the daily station records by the variance ratio of projected monthly precipitation between the two periods.

Projected mean maximum and minimum temperature shifts were directly added to the corresponding baseline monthly means. New daily temperature variance was calculated by multiplying the baseline variance of daily temperature by the calculated variance ratio of monthly mean temperature. All new parameter values were then input into CLIGEN, and 100 years of daily weather data were generated for each climate change scenario.

In general, newly generated average annual precipitation was several percent points greater than the projected or downscaled target annual average for both methods and three climate change scenarios. Thus, the initially adjusted mean daily precipitation by Eq. 3 was further scaled down for all 12 months to match the target value. The overestimation might have resulted from model approximation and interactive effects of a general increase in precipitation variance and a skewed normal distribution of daily precipitation employed in CLIGEN. More information on testing and evaluation of both methods can be found in Zhang et al. (2004) and Zhang (2005).

### 2.6 Impact simulation

All measured soil properties including saturated hydraulic conductivity (3.7 mm $h^{-1}$ in the top 20-cm layer) and the two runoff plots (20 m long, 8.7 and 17.6% slope), which were used in the WEPP model calibration, were used in the climatic impact simulation. Overall mean of measured storm duration at Changwu was 2.88 times that of CLIGEN-generated storm durations. To offset this bias, a factor of 2.88 was multiplied to CLIGEN-generated storm durations and relative peak intensities (ratio of instant peak rainfall intensity to average storm intensity) in both baseline and changed climates (Zhang and Liu 2005). A common regional three-year rotation of wheat–wheat–maize was simulated. In the simulation under the baseline climate condition, winter wheat was planted on September 23 and harvested on June 27 of the following year; and maize was planted on April 15 and harvested on September 22. However, under the changed climates, wheat was planted 3 days later and harvested 3 days earlier; and maize was planted 3 days earlier and harvested 4 days earlier to accommodate the increased temperature. Conventional tillage and residue management systems were simulated. About 90% of crop residue was removed and field was moldboard plowed one week after harvest. Based on the emissions scenarios of A2, B2, and GGa, the corresponding $CO_2$ concentrations in the atmosphere by 2025 would be 592, 416, and 444 ppmv, which were used in the WEPP simulation.

**Fig. 1** **a** Historical mean monthly precipitation at Changwu during 1957–2001, **b** ratio of mean monthly precipitation of 2010–2039 to that of 1950–1999 under GGa1 estimated using the explicit and implicit spatial downscaling methods for Changwu, and **c** variance ratio of monthly precipitation of 2010–2039 to that of 1950–1999 (Note the *horizontal line at 1* indicates no change between the two periods, *greater than 1* an increase, and *less than 1* a decrease)

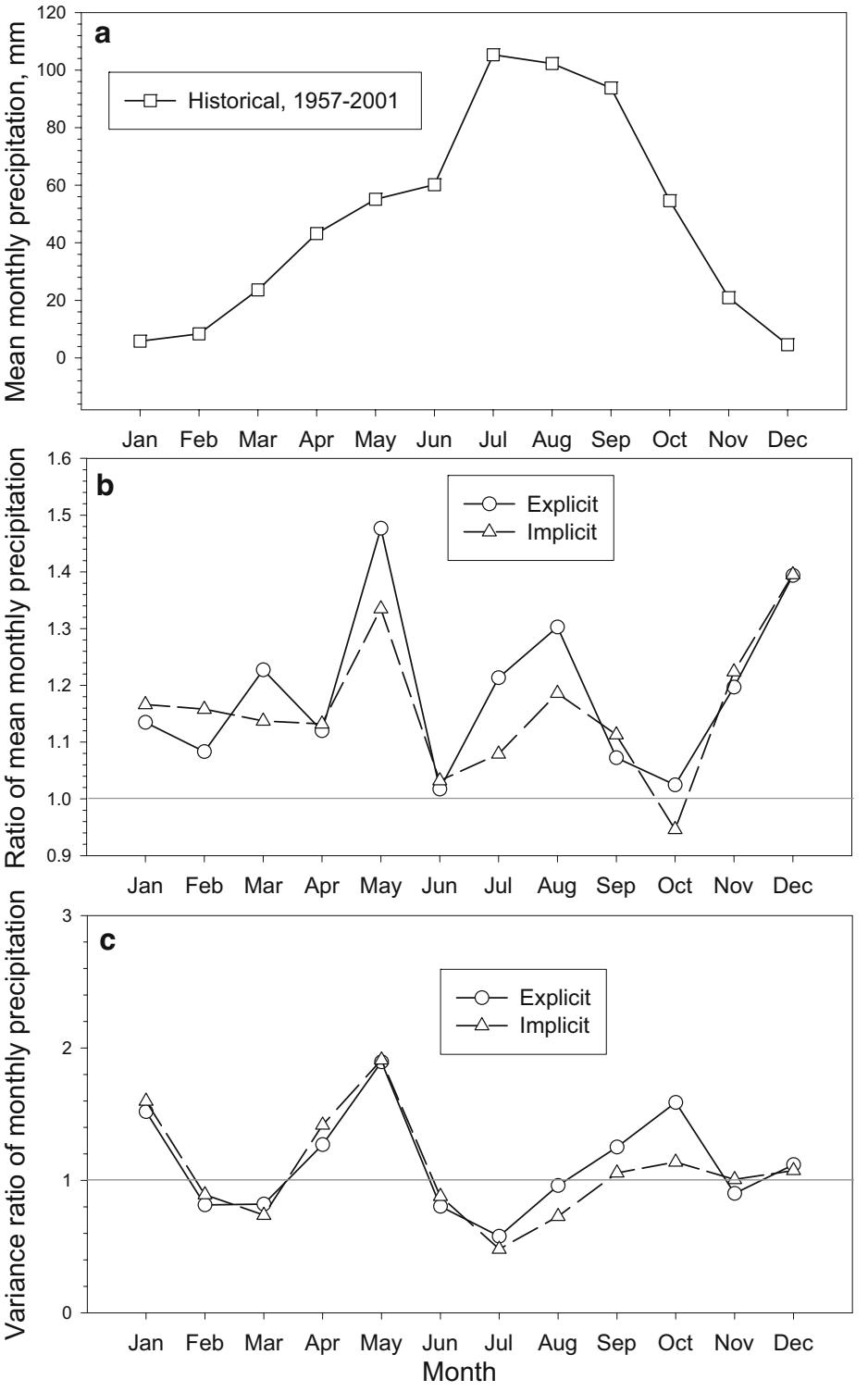
a
Historical, 1957-2001
Mean monthly precipitation, mm
120
100
80
60
40
20
0
Jan Feb Mar Apr May Jun Jul Aug Sep Oct Nov Dec
b
Explicit
Implicit
Ratio of mean monthly precipitation
1.6
1.5
1.4
1.3
1.2
1.1
1.0
0.9
Jan Feb Mar Apr May Jun Jul Aug Sep Oct Nov Dec
c
Explicit
Implicit
Variance ratio of monthly precipitation
3
2
1
0
Jan Feb Mar Apr May Jun Jul Aug Sep Oct Nov Dec
Month

The WEPP model was run for 100 years at two slopes for both baseline and six climate scenarios downscaled using explicit and implicit methods. The contrasts of simulated annual output between the two methods were tested for statistical significance using a nonparametric test of Kolmogorov-Smirnov (K-S). The K-S test, which is applicable to any distribution, was used to test the null hypothesis that the two distributions in each contrast are identical.

## 3 Results and discussion

### 3.1 Comparison of downscaled monthly projections

#### *3.1.1 Climate scenario GGa1*

Explicitly and implicitly downscaled means and variance ratios of monthly precipitation of the GGa1 climate change scenario are shown in Fig. 1 for Changwu. Historical mean monthly precipitation during 1957–2001 at Changwu is also presented in Fig. 1a, showing that the primary rainy season in the region is in the summer during which most severe storms and soil erosion events occur. Overall, both methods predicted precipitation increases for almost all the months. The seasonal patterns of the monthly precipitation means estimated by both methods were similar, with the explicit method predicting slightly more precipitation, especially in May, July, and August (Fig. 1b). The variance ratios of monthly precipitation estimated by both methods agreed very well for all months except August, September, and October (Fig. 1c). The explicit method estimated greater variance in this period, which would have important implications in terms of soil loss and runoff predictions as is shown later.

Temperature shifts and variance ratios estimated by the two methods are contrasted in Fig. 2 for maximum temperature and in Fig. 3 for minimum temperature. The shifts in maximum temperature estimated by the explicit method were lower than those estimated by the implicit method for all the seasons except the winter (January, February, and March); however, the seasonal trends of variance changes were rather similar (Fig. 2). The shifts in minimum temperature estimated by the explicit method were consistently higher than those by the implicit method for all the months except January; but, the variance ratios of the two methods followed a similar pattern closely (Fig. 3).

#### *3.1.2 Climate scenario B2a*

Monthly precipitation of climate change scenario B2a, as compared to the present climate, would increase for most months at Changwu, and the increases estimated by the explicit method were similar to those estimated by the implicit method for most months (Fig. 4a). The seasonal patterns of the variance ratios by both methods were also similar, showing an overall increase in variability under the climate change, but the explicit method tended to predict greater variability than did the implicit method for March, July, and December (Fig. 4b). There were no consistent biases between the two methods in terms of both shifts and variance ratios for maximum temperature (Fig. 5). In contrast, the shifts in minimum temperature estimated by the explicit method were higher than those by the implicit method for all months except January (Fig. 6a). The month-to-month fluctuations of the variance ratios of minimum temperature estimated by both methods were similar except September, October, and November (Fig. 6b).

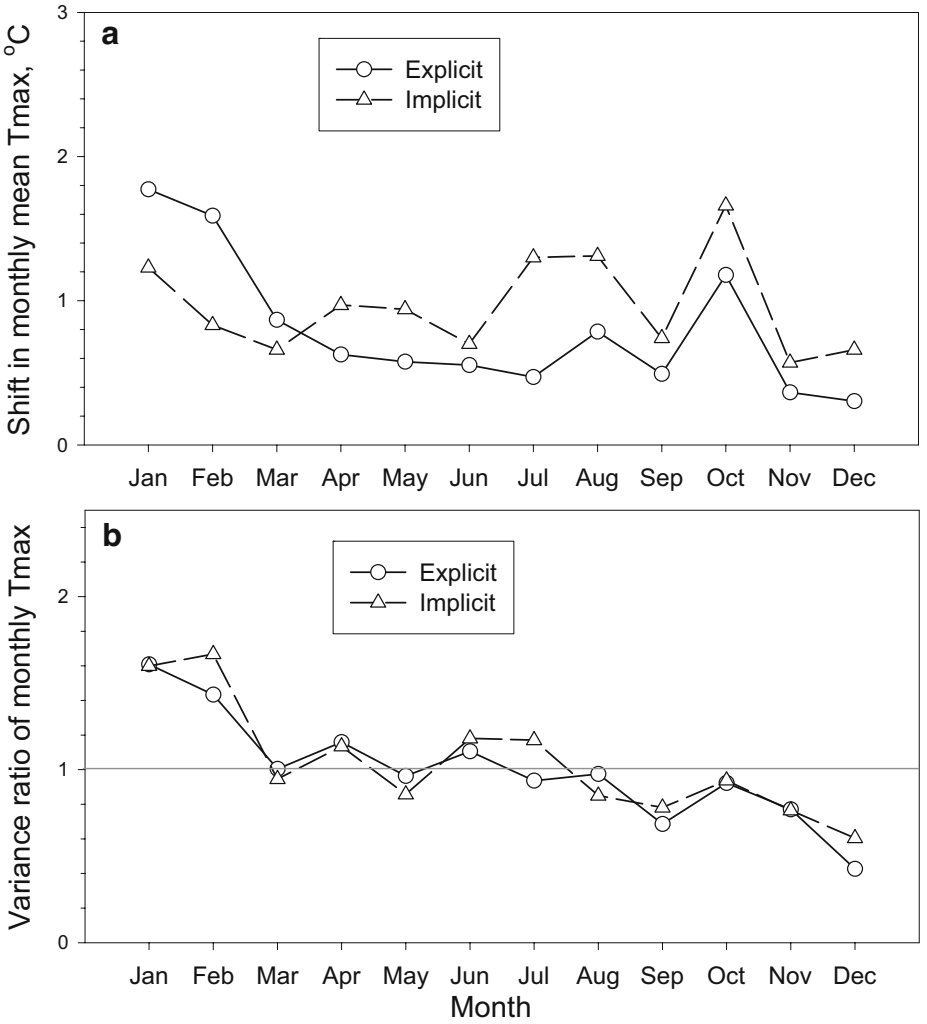


**Fig. 2** **a** Maximum temperature shift between 2010–2039 and 1950–1999, and **b** variance ratio of monthly mean maximum temperature ($T_{max}$) of 2010–2039 to that of 1950–1999 under GGa1 estimated using the explicit and implicit downscaling methods for Changwu (Note the *horizontal line at 1* indicates no change between the two periods, *greater than 1* an increase, and *less than 1* a decrease)

### *3.1.3 Climate scenario A2a*

Although monthly mean precipitation estimated by both methods followed a similar seasonal pattern, greater increases were estimated by the implicit method, especially for September and October (Fig. 7a). Variance ratios of monthly precipitation estimated by the implicit method were greater than those estimated by the explicit method for most months, especially for October (Fig. 7b). The greater increases in monthly precipitation means and variances in September and October with the implicit method were because a few extremely large monthly precipitation totals were projected for the 2 months by HadCM3 and those

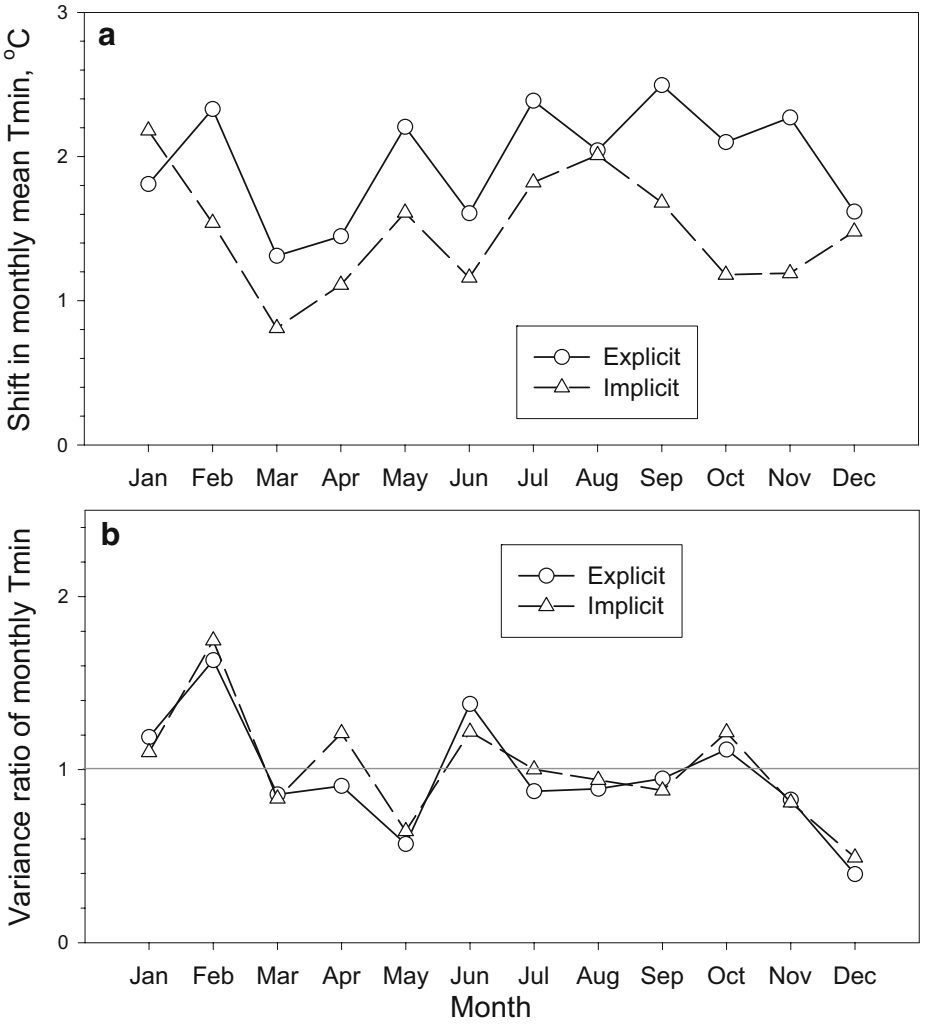


**Fig. 3** **a** Minimum temperature shift between 2010–2039 and 1950–1999, and **b** variance ratio of monthly mean minimum temperature ($T_{min}$) of 2010–2039 to that of 1950–1999 under GGa1 estimated using the explicit and implicit downscaling methods for Changwu

extremes were directly used in computing variance ratios and precipitation means in the implicit method while the transformed data were used in the explicit method. The shifts and variance ratios of maximum temperature estimated by both methods followed similar seasonal patterns well (Fig. 8). Similar to scenarios GGa1 and B2a, the shifts in minimum temperature estimated by the explicit methods were consistently higher than those estimated by the implicit method for most months (Fig. 9a). However, the month-to-month fluctuations of variance ratios estimated by both methods were rather similar (Fig. 9b).

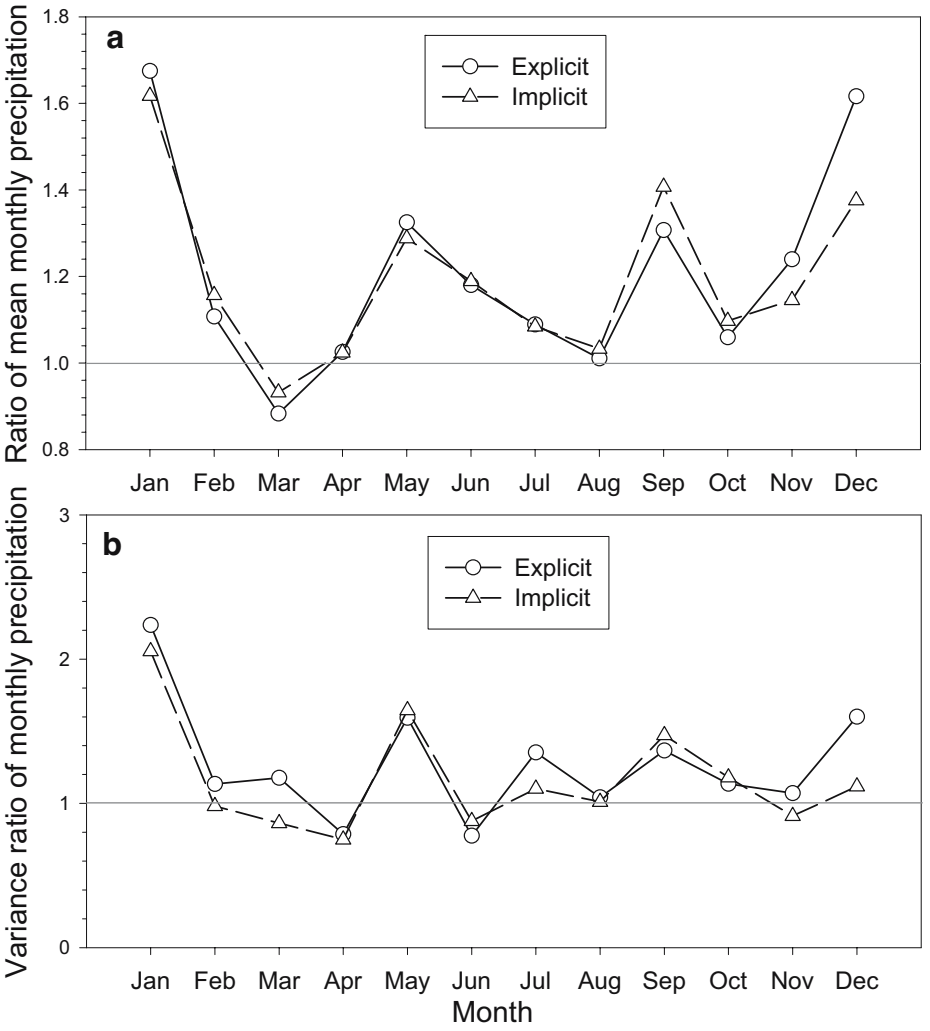


**Fig. 4** **a** Ratio of mean monthly precipitation of 2010–2039 to that of 1950–1999, and **b** variance ratio of monthly precipitation of 2010–2039 to that of 1950–1999 under B2a estimated using the explicit and implicit downscaling methods for Changwu

### 3.2 Difference in generated daily weather series

Precipitation and temperature means and variances of explicitly and implicitly downscaled monthly values (Figs. 1, 2, 3, 4, 5, 6, 7, 8 and 9) have to be incorporated or disaggregated to daily time series using CLIGEN. During disaggregation, daily precipitation variance was estimated using Eq. 4 in the explicit method, while it was estimated by directly multiplying the baseline daily variance by the monthly variance ratio in the implicit method. Such proportional adjustment was justified because monthly precipitation variances under climate changes at the Changwu station were not known without an explicit spatial downscaling. As

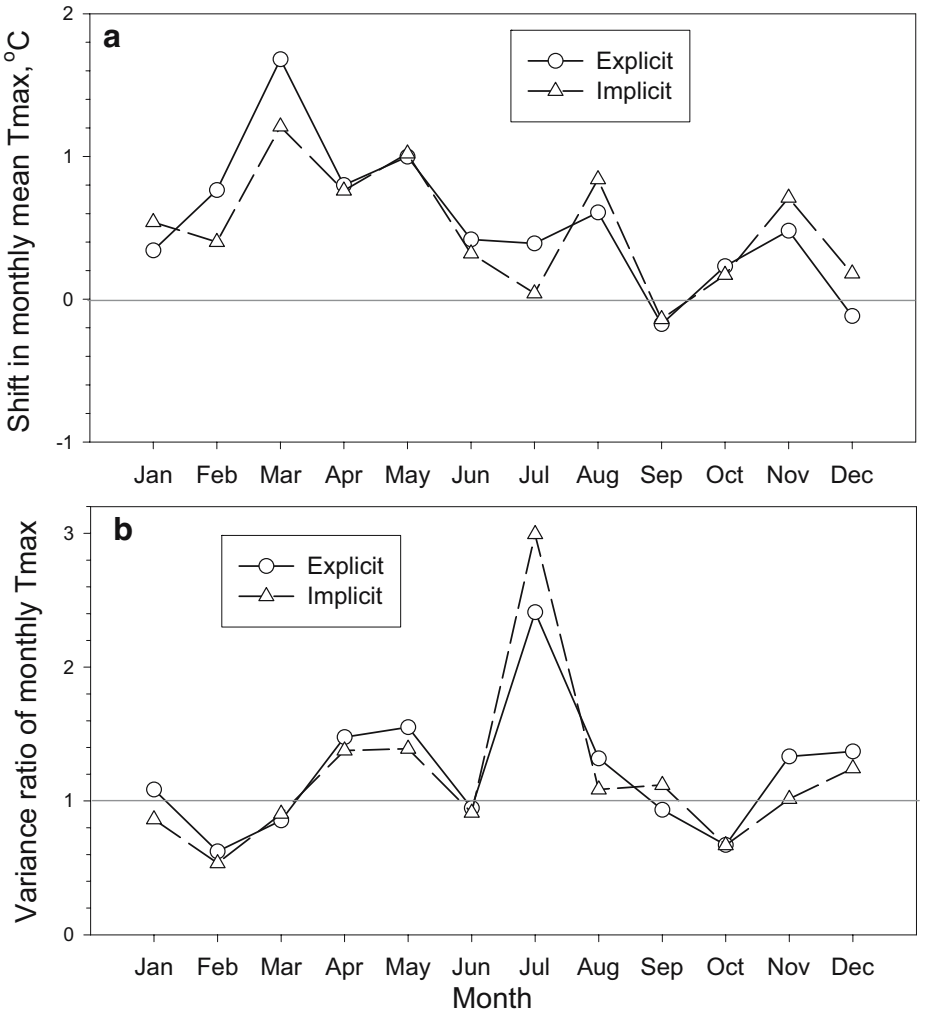


**Fig. 5** **a** Maximum temperature shift between 2010–2039 and 1950–1999, and **b** variance ratio of monthly mean maximum temperature ($T_{max}$) of 2010–2039 to that of 1950–1999 under B2a estimated using the explicit and implicit downscaling methods for Changwu

noted by Zhang et al. (2004), this proportional adjustment would tend to underestimate variance of daily precipitation and consequently variance of monthly precipitation. The underestimation of daily precipitation variance would have significant consequences on runoff and soil loss prediction. Greater daily precipitation variance leads to a greater number of heavier storms in the generated daily weather. Heavier storms, as generated by CLIGEN, often have greater peak rainfall intensities during storms. This is because peak intensity is positively related to storm depth by a two-parameter gamma distribution in CLIGEN. Thus, greater daily precipitation variance would lead to greater runoff and soil loss. Except for precipitation variance, all other variables including temperature mean and variance, daily precipitation mean, and conditional probabilities of precipitation occurrence ($P_{w/w}$ and $P_{w/d}$) were estimated using the same procedure or equations in both methods. It is very likely that

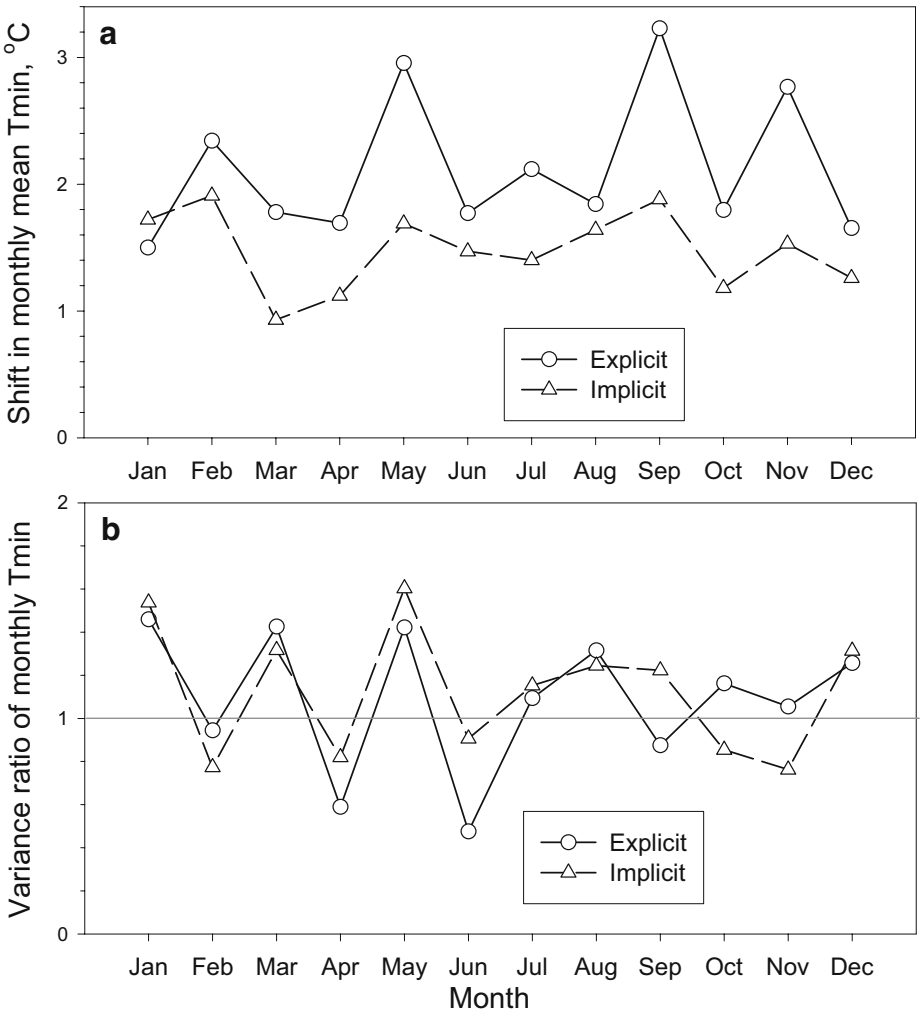


**Fig. 6** **a** Minimum temperature shift between 2010–2039 and 1950–1999, and **b** variance ratio of monthly mean minimum temperature ($T_{min}$) of 2010–2039 to that of 1950–1999 under B2a estimated using the explicit and implicit downscaling methods for Changwu

the differences between the two downscaling methods as presented in Figs. 1, 2, 3, 4, 5, 6, 7, 8 and 9 for the monthly values would be amplified in the generated daily time series, especially as far as precipitation variability is concerned.

### 3.3 Averaged annual climate change

Explicit and implicit methods predicted a general increase in both annual precipitation amounts and variability at Changwu during 2010–2039 for all three climate change scenarios (Table 2). Compared with the explicit method, 15.6 and 2.0% more precipitation (percent of the baseline) were predicted by the implicit method for the A2a and B2a climate scenarios, respectively, and 4.9% lesser precipitation for GGa1. The large discrepancy

between the two methods indicated the potential effect of downscaling methods on downscaled climate scenarios and the importance of using appropriate downscaling technique for impact assessments. The averaged variance ratios of monthly precipitation were also influenced by the downscaling methods. As mentioned earlier, precipitation variance has a great effect on predicted runoff and soil loss.

Average temperature increases during 2010–2039 would range from 0.5 to 1.0°C for maximum temperature and 1.5 to 2.3°C for minimum temperature (Table 2). The average monthly variances under climate change would be slightly greater than those of present climate for both maximum and minimum temperatures. Overall, the average increases in maximum temperature predicted by both methods were relatively close; however, the average increases in minimum temperature estimated by the explicit method tended to be

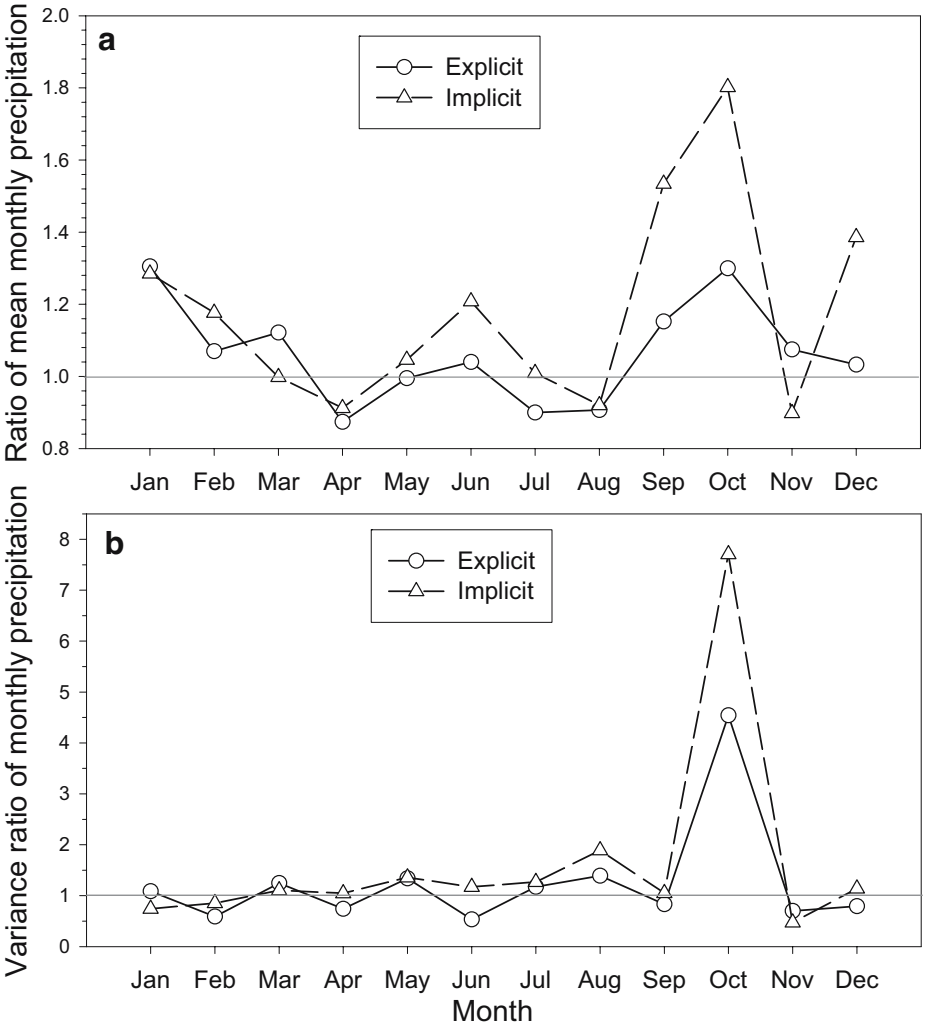


**Fig. 7** **a** Ratio of mean monthly precipitation of 2010–2039 to that of 1950–1999, and **b** variance ratio of monthly precipitation of 2010–2039 to that of 1950–1999 under A2a estimated using the explicit and implicit downscaling methods for Changwu

higher than those estimated by the implicit method. These results further underscore the need of using appropriate downscaling methods for more accurate impact assessments.

### 3.4 Impact on runoff and soil erosion

#### *3.4.1 Long-term impact*

Predicted average annual precipitation, runoff, and soil loss during 2010–2039 are presented in Table 3. Note that the percent precipitation increases in Table 3 are slightly different from those in Table 2. The values in Table 2 are the target changes calculated using spatially downscaled GCM projections, while those in Table 3 are calculated using

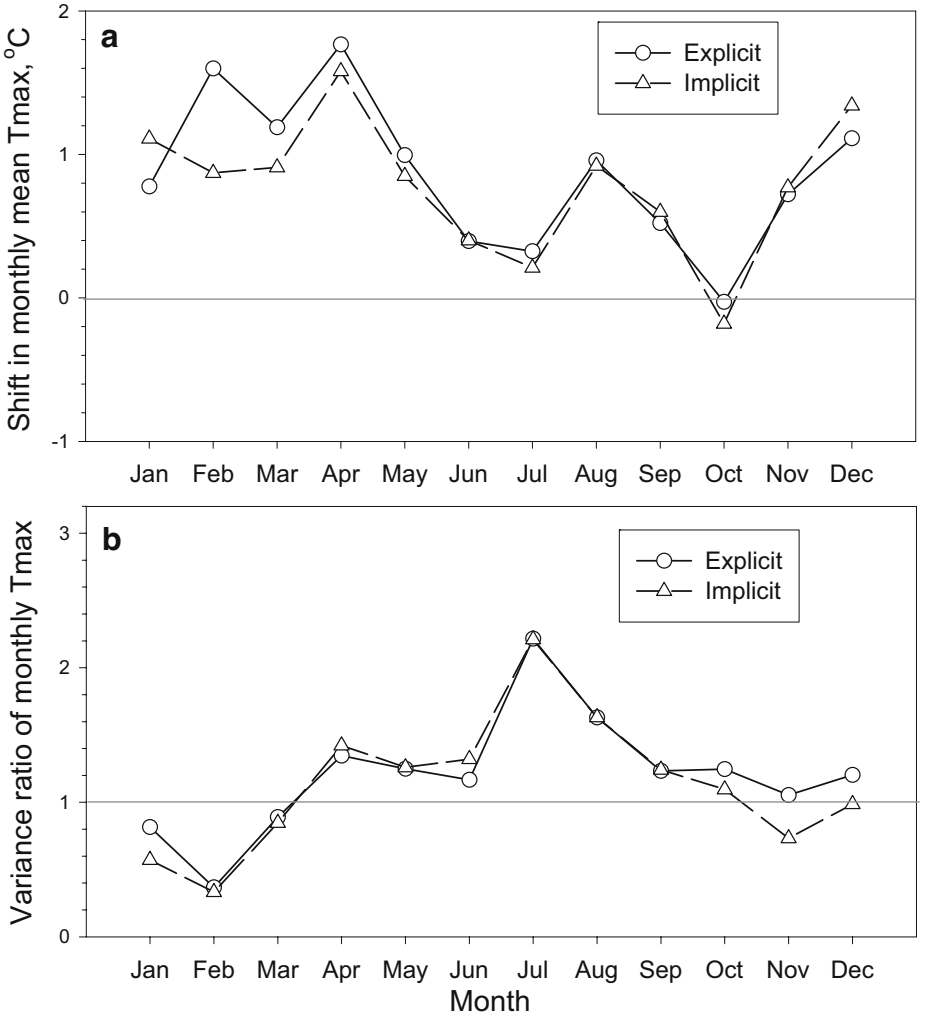


**Fig. 8** **a** Maximum temperature shift between 2010–2039 and 1950–1999, and **b** variance ratio of monthly mean maximum temperature ($T_{max}$) of 2010–2039 to that of 1950–1999 under A2a estimated using the explicit and implicit downscaling methods for Changwu

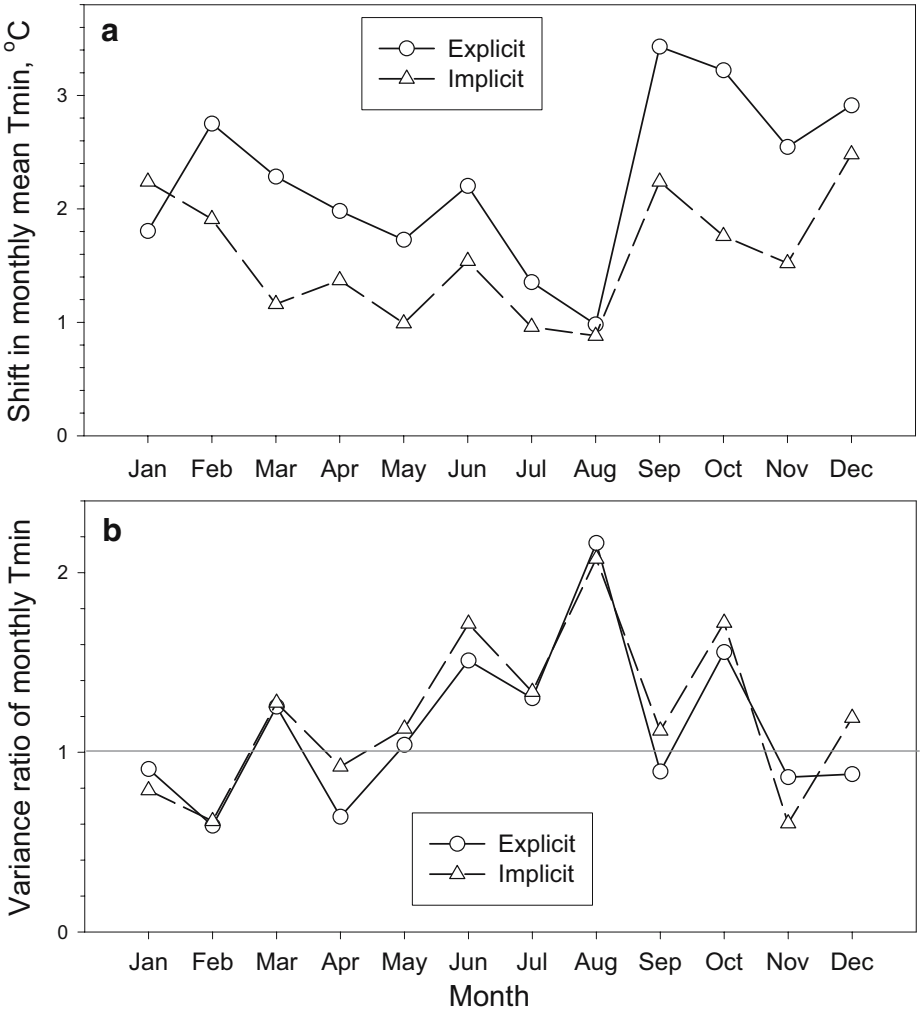


**Fig. 9** **a** Minimum temperature shift between 2010–2039 and 1950–1999, and **b** variance ratio of monthly mean minimum temperature ($T_{min}$) of 2010–2039 to that of 1950–1999 under A2a estimated using the explicit and implicit downscaling methods for Changwu

CLIGEN-generated daily weather data. Compared with the runoff depth under the baseline climate, runoff depths increased by 6–112% for all climate scenarios. The sensitivity of runoff increase to precipitation increase under climate change was heavily influenced by the downscaling methods. Runoff distributions with the explicit method significantly shifted to higher values compared with the implicit method under Ba2 and GGa1 at $P$=0.001 (Table 3). However, no difference was detected for A2a. This is because runoff increases due to increases in precipitation variance were largely offset by runoff decreases due to precipitation decreases predicted with the explicit method. For a 1% increase in precipitation, percent increases in runoff were 3–6 times greater in the explicit downscaling than those in the implicit downscaling for all climate scenarios. This is because the implicit method tends to underestimate daily precipitation variance. For a similar median value,

**Table 2** Averaged annual climate changes of explicit and implicit spatial downscaling between 1950–1999 and 2010–2039

| Climate scenario | Spatial downscaling | Precipitation | | Maximum temperature | | Minimum temperature | |
|---|---|---|---|---|---|---|---|
| | | Change (%) | M.V.R.[a] | Shift (°C) | M.V.R. | Shift (°C) | M.V.R. |
| A2a | Explicit | 1.8 | 1.25 | 0.86 | 1.08 | 2.27 | 1.13 |
| | Implicit | 17.4 | 1.65 | 0.78 | 1.21 | 1.59 | 1.14 |
| B2a | Explicit | 13.9 | 1.27 | 0.54 | 1.22 | 2.12 | 1.09 |
| | Implicit | 15.9 | 1.16 | 0.50 | 1.18 | 1.48 | 1.13 |
| GGa1 | Explicit | 17.5 | 1.13 | 0.80 | 1.00 | 1.97 | 0.97 |
| | Implicit | 12.6 | 1.08 | 0.96 | 1.04 | 1.48 | 1.01 |

[a] M.V.R.=average monthly variance ratio of 2010–39 over 1957–2001.

lesser precipitation variances mean fewer heavy storms and lower peak rainfall intensities, which often lead to smaller portions of rainwater to run off.

Due to the increases in runoff depths, annual average soil loss rates during 2010–2039, compared with those under the baseline climate, increased by 18–167% for all cases except the implicit method of the GGa1 scenario (Table 3). The decrease in soil loss under GGa1 might be caused by the decreases of monthly precipitation variances estimated by the implicit method for July and August during which most soil erosion occurred in the region as well as

**Table 3** Predicted mean annual precipitation, runoff, and soil loss during 2010–2039 as well as their percent changes relative to the corresponding slope in the baseline scenario for Changwu, China under conventional tillage in a wheat–wheat–maize rotation for three climate change scenarios following explicit or implicit spatial downscaling[a]

| Slope (%) | Spatial downscaling | Precipitation | | Runoff | | Soil loss | |
|---|---|---|---|---|---|---|---|
| | | Depth (mm) | Change (%) | Depth (mm) | Change (%) | Rate (t ha$^{-1}$) | Change (%) |
| Baseline scenario of Changwu Station at 350 ppmv $CO_2$ | | | | | | | |
| 8.7 | Station | 579 | 0 | 45 | 0 | 3.2 | 0 |
| 17.6 | Station | 579 | 0 | 55 | 0 | 9.5 | 0 |
| Scenario A2a at 592 ppmv $CO_2$ | | | | | | | |
| 8.7 | Implicit | 683[b] | 18 | 82 | 82 | 5.3[d] | 69 |
| 8.7 | Explicit | 604 | 4 | 96 | 112 | 8.4 | 167 |
| 17.6 | Implicit | 683 | 18 | 94 | 71 | 14.8[c] | 56 |
| 17.6 | Explicit | 604 | 4 | 107 | 96 | 22.1 | 133 |
| Scenario B2a at 416 ppmv $CO_2$ | | | | | | | |
| 8.7 | Implicit | 673 | 16 | 58[b] | 29 | 4.0[d] | 26 |
| 8.7 | Explicit | 662 | 14 | 82 | 81 | 6.2 | 96 |
| 17.6 | Implicit | 673 | 16 | 69[b] | 26 | 11.1[c] | 18 |
| 17.6 | Explicit | 662 | 14 | 93 | 70 | 17.0 | 80 |
| Scenario GGa1 at 444 ppmv $CO_2$ | | | | | | | |
| 8.7 | Implicit | 652 | 12 | 48[b] | 6 | 2.9[c] | −8 |
| 8.7 | Explicit | 685 | 18 | 72 | 60 | 4.7 | 49 |
| 17.6 | Implicit | 652 | 12 | 58[c] | 6 | 8.5[c] | −10 |
| 17.6 | Explicit | 685 | 18 | 82 | 49 | 12.4 | 31 |

[a] Ninety percent residue was removed and soil was moldboard plowed within one week after each harvest in a wheat–wheat–maize rotation; [b, c, d] significantly different for the Implicit–Explicit contrast at the given slope at $P$=0.001, 0.01, and 0.05, respectively, using the K-S test.

by better maize growth in the period under climate change. Distributions of soil loss rates estimated with the explicit method shifted significantly to higher values compared with the implicit method for all cases at $P<0.05$. For a 1% increase in precipitation, percent increases in soil loss were 4–10 times greater with the explicit method than those with the implicit method under the A2a and B2a scenarios. More dramatic changes were seen under the GGa1 scenario where soil loss rates, compared with the baseline, were decreased by 8–10% with the implicit method while they were increased by 31–49% with the explicit method. Overall, soil loss changes were more sensitive than runoff to precipitation changes for both downscaling methods. This result is consistent with the finding of Nearing et al. (2005), who concluded that soil erosion was likely to be more affected than runoff by changes in rainfall.

### *3.4.2 Distribution of event soil loss for erosion-prone months*

As is shown in Fig. 1a, the rainy season is between July and September in the region, during which most severe erosion occurs. Soil loss measured in field plots at Changwu during 1988–1992 showed that more than 98% of total soil loss was from July and August. The severe erosion in this period was a result of occurrence of large convective storms and unprotected soil in the conventional tillage under winter wheat production. In order to examine the effects of the downscaling methods on event soil loss prediction, probability distributions of simulated event soil loss in most erosive months are shown in Figs. 10, 11, and 12 for the three climate change scenarios. Soil losses for the period of July–October

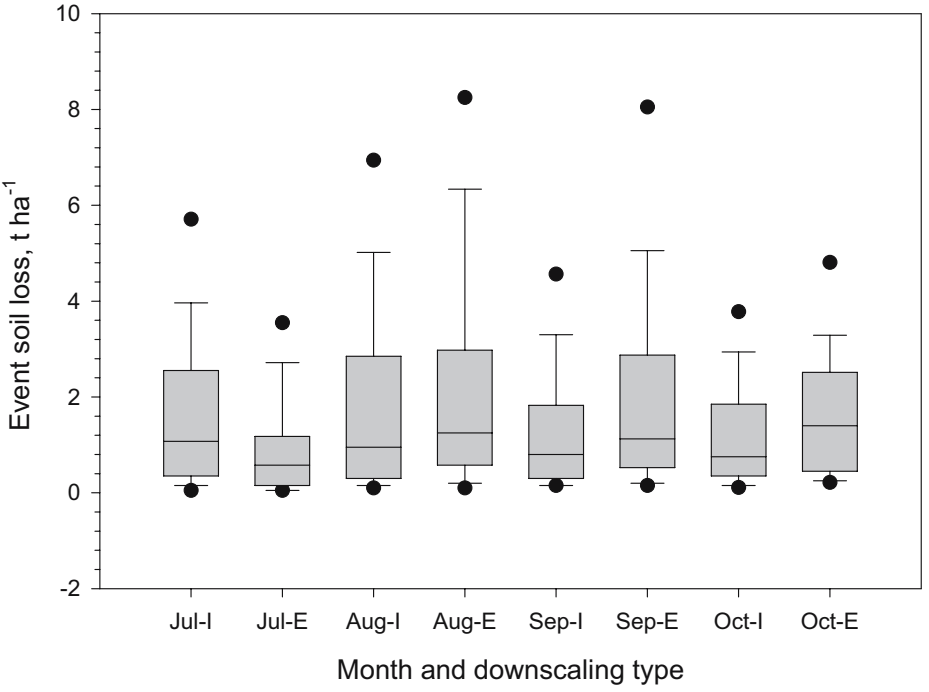


**Fig. 10** Box plot of simulated event soil loss on a 17.6% slope in a wheat–wheat–corn rotation under conventional tillage for four summer months using the implicit (*I*) and explicit (*E*) methods under GGa1. (95th, 90th, 75th, 50th, 25th, 10th, and 5th percentiles are shown by *upper solid circle*, *upper whisker*, *upper box border*, *middle horizontal line*, *lower box border*, *lower whisker* and *solid circle*, respectively)

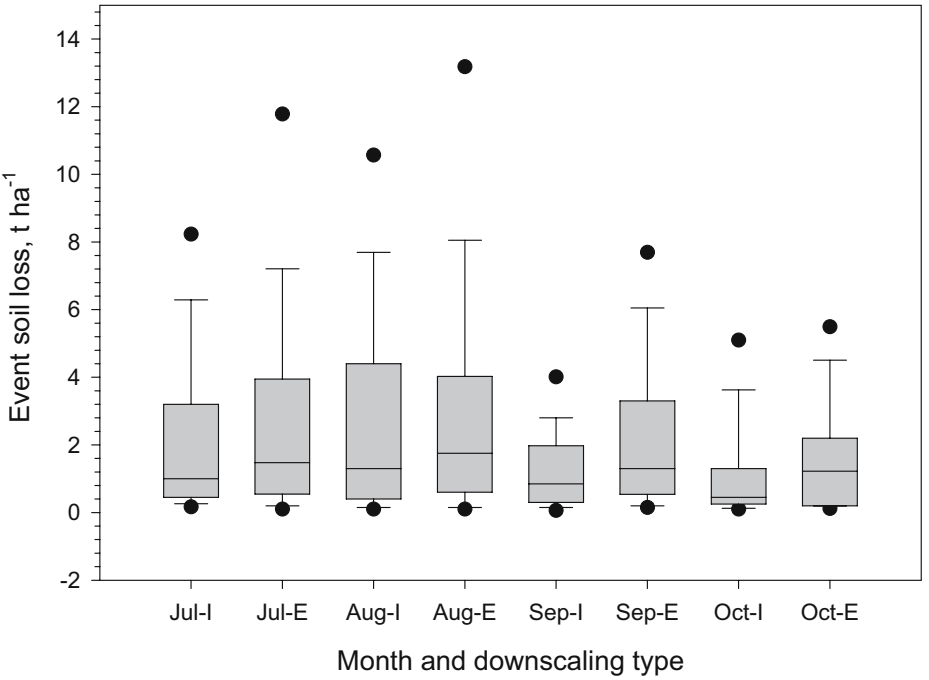


**Fig. 11** Box plot of simulated event soil loss on a 17.6% slope in a wheat–wheat–corn rotation under conventional tillage for four summer months using the implicit (*I*) and explicit (*E*) methods under B2a. (95th, 90th, 75th, 50th, 25th, 10th, and 5th percentiles are shown by *upper solid circle*, *upper whisker*, *upper box border*, *middle horizontal line*, *lower box border*, *lower whisker* and *solid circle*, respectively)

estimated with the implicit method (explicit method) accounted for 84 (86), 88 (94), and 93% (97) of total annual soil losses for GGa1, B2a, and A2a, respectively. Since most soil losses occurred in the selected months, any conclusion drawn from Figs. 10, 11 and 12 should be representative of and applicable to total annual soil loss. Under GGa1, event soil losses at the 50th, 75th, 90th, and 95th percentiles estimated with the explicit method were greater than the corresponding soil losses estimated with the implicit method in all months but July (Fig. 10), indicating much greater variability in simulated event soil loss associated with the explicit method. This result is consistent with the fact that soil loss is very sensitive to daily precipitation variability and the implicit method tends to underestimate it. Similar trends are shown in Figs. 11 and 12 for B2a and A2a, respectively, in which event soil losses at the four percentiles were consistently greater with the explicit method for all four months. The contrasting soil loss distributions between the two downscaling methods indicate the importance of appropriately handling precipitation variance in predicting climatic impacts on soil erosion.

## 3.5 Impact on soil water balance and crop yield

### *3.5.1 Soil water balance*

Predicted mean annual plant transpiration, soil evaporation, long-term soil moisture reserve in the 1.8-m soil profile, and wheat and maize grain yields under the conventional tillage

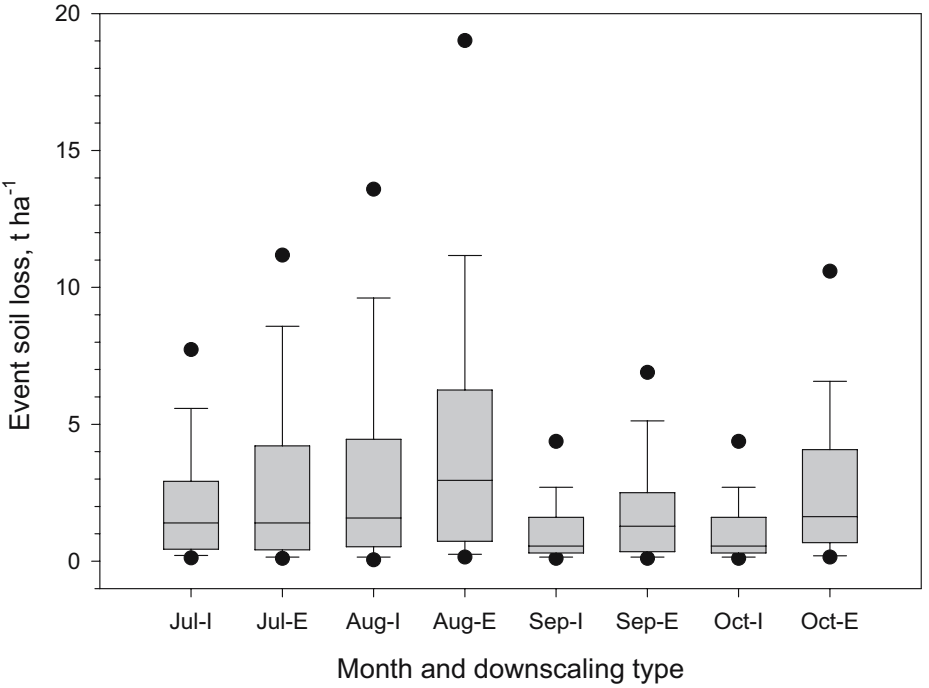


**Fig. 12** Box plot of simulated event soil loss on a 17.6% slope in a wheat–wheat–corn rotation under conventional tillage for four summer months using the implicit (*I*) and explicit (*E*) methods under A2a. (95th, 90th, 75th, 50th, 25th, 10th, and 5th percentiles are shown by *upper solid circle*, *upper whisker*, *upper box border*, *middle horizontal line*, *lower box border*, *lower whisker* and *solid circle*, respectively)

are shown in Table 4. Compared with the baseline conditions, plant transpiration, as a result of overall increases in annual precipitation, increased from 12 to 19% for all scenarios and downscaling methods except the explicit method under A2a. The decrease in A2a with the explicit method was because the annual precipitation increase (25 mm) was less than the average runoff increase (45 mm, Table 3) as a result of an increase in precipitation variance that led to an increase in number of heavy storms. Similar to plant transpiration, average annual soil evaporation, compared with the baseline, increased in all cases but the explicit method of A2a. The increases ranged from 2 to 12%, with a tendency that the percent increases with the explicit method were smaller than those with the implicit method for three climate scenarios. Long-term average soil water reserve in the 1.8-m soil profile under climate changes increased by 1–7% except the explicit method of A2a. The increased soil moisture reserve is an integrated effect of all hydrological changes in the agro-ecosystem. Overall, simulated distributions of transpiration, soil evaporation, and soil moisture reserve with the explicit method are significantly different from those with the implicit method for A2a, because significant difference in precipitation between the two methods was detected for A2a. Significant differences in distributions were also found for soil evaporation at the 17.6% slope and for soil moisture at both slopes under B2a. Simulated results showed that less than 1.5-mm water, on average, was percolated below the 1.8-m depth each year, and less than 0.3-mm laterally transported downslope. In addition, slope steepness had negligible effect on plant transpiration, soil evaporation, and soil moisture balance in this study.

**Table 4** Predicted mean annual transpiration, soil evaporation, average daily soil moisture in 1.8-m soil profile, wheat and maize grain yields during 2010–2039 as well as their percent changes relative to the corresponding slope in the baseline scenario for Changwu, China under conventional tillage in a wheat–wheat–maize rotation for three climate change scenarios following explicit or implicit spatial downscaling[a]

| Slope (%) | Spatial downscaling | Transpiration | | Soil evaporation | | Soil moisture | | Wheat | | Maize | |
|---|---|---|---|---|---|---|---|---|---|---|---|
| | | Depth (mm) | Change (%) | Depth (mm) | Change (%) | Depth (mm) | Change (%) | Yield (t ha$^{-1}$) | Change (%) | Yield (t ha$^{-1}$) | Change (%) |
| Baseline scenario of Changwu Station at 350 ppmv $CO_2$ | | | | | | | | | | | |
| 8.7 | Station | 353 | 0 | 183 | 0 | 301 | 0 | 2.9 | 0 | 7.0 | 0 |
| 17.6 | Station | 348 | 0 | 179 | 0 | 297 | 0 | 2.8 | 0 | 6.8 | 0 |
| Scenario A2a at 592 ppmv $CO_2$ | | | | | | | | | | | |
| 8.7 | Implicit | 397[b] | 12 | 205[b] | 12 | 324[b] | 7 | 3.8[c] | 31 | 10.2[c] | 45 |
| 8.7 | Explicit | 339 | −4 | 171 | −7 | 289 | −4 | 2.9 | −1 | 8.0 | 15 |
| 17.6 | Implicit | 390[b] | 12 | 201[b] | 12 | 318[b] | 7 | 3.6[c] | 30 | 9.9[c] | 45 |
| 17.6 | Explicit | 332 | −5 | 166 | −7 | 285 | −4 | 2.8 | −1 | 7.8 | 14 |
| Scenario B2a at 416 ppmv $CO_2$ | | | | | | | | | | | |
| 8.7 | Implicit | 412 | 17 | 205 | 12 | 322[d] | 7 | 3.8 | 31 | 9.2 | 32 |
| 8.7 | Explicit | 396 | 12 | 187 | 2 | 305 | 1 | 3.5 | 23 | 8.6 | 23 |
| 17.6 | Implicit | 405 | 16 | 201[d] | 12 | 318[d] | 7 | 3.6 | 30 | 9.1 | 33 |
| 17.6 | Explicit | 389 | 12 | 182 | 2 | 300 | 1 | 3.4 | 22 | 8.3 | 22 |
| Scenario Gga1 at 444 ppmv $CO_2$ | | | | | | | | | | | |
| 8.7 | Implicit | 406 | 15 | 199 | 9 | 311 | 3 | 3.8 | 31 | 9.6 | 37 |
| 8.7 | Explicit | 419 | 18 | 196 | 7 | 312 | 4 | 4.1 | 41 | 9.6 | 37 |
| 17.6 | Implicit | 400 | 15 | 195 | 9 | 307 | 4 | 3.7 | 31 | 9.4 | 38 |
| 17.6 | Explicit | 413 | 19 | 192 | 7 | 308 | 4 | 3.9 | 41 | 9.5 | 38 |

[a] Ninety percent residue was removed and soil was moldboard plowed within one week after each harvest in a wheat–wheat–maize rotation. On average, less than 1.5-mm water was percolated below the 1.8-m soil profile, and less than 0.3-mm water was laterally transported downslope each year; [b, c, d] significantly different for the Implicit–Explicit contrast at the given slope at $P$=0.001, 0.01, and 0.05, respectively, using the K-S test.

### *3.5.2 Grain yield*

Simulated percent increases in wheat grain yield under climate change, compared to the baseline, ranged from 22 to 41% for all cases except the explicit method of A2a (Table 4). In general, the percent increases in yield corresponded well to the increases in precipitation, plant transpiration, and $CO_2$ concentration, as well as the negative effect of temperature rise. The significant difference in yield distributions between the two methods was diagnosed only for A2a. The 1% decrease in the explicit method, in contrast to the 31% increase in the implicit method, was an integrated result of greater water deficit (Table 4) and a 0.38°C more increase in annual mean temperature under A2a (Table 2). Water is the limiting factor for crop production in the region, and therefore any difference in precipitation will considerably affect crop yields. As for the temperature effect, Zhang et al. (2004) reported that simulated wheat yield decreased by some 8% for a 1°C increase in growing-season mean temperature in Oklahoma, USA. Mearns et al. (1997) evaluated wheat yield sensitivity to temperature in Kansas, USA, and reported a 10–12% decrease in yield for 1°C increase in mean annual temperature. In the B2a scenario, the yield was numerically about 8% higher with the implicit method than with the explicit method, resulting from a greater increase in soil water and a 0.34°C less increase in mean

temperature with the implicit method. The 10% more increase with the explicit method relative to the implicit method under GGa1 was mainly attributed to the increase in soil water because the mean temperatures predicted by the two methods were similar. Although there were numerical differences in mean yields between the two downscaling methods for B2a and GGa1, their yield distributions were not significantly different from one another.

Similar to wheat, maize yields corresponded well to increases in precipitation, soil water, and $CO_2$ concentration in all scenarios (Table 4). However, the responses were somewhat different between the two crops, reflecting the effects of seasonal variations in downscaled temperature and precipitation on crop yield. For example, the 15% increase in maize yield with the explicit method under A2a, in contrast to the 1% decrease in wheat, might be caused by lesser temperature rise and more precipitation increases in summer than in winter (Figs. 7, 8 and 9). The largest increase in maize yield with the implicit method under A2a was a result of greater increases in precipitation and $CO_2$ concentration and a moderate increase in mean temperature, as compared to the other scenarios. The maize yield with the implicit method was some 10% greater than that with the explicit method under B2a, because a greater precipitation increase and a lesser temperature rise were predicted by the implicit method. There was little difference in the maize yields between the two methods under GGa1, though some 10% difference was found in wheat yields, again showing seasonality of crop response to climatic change. Similar to wheat, differences in yield distributions between the two methods were significant for A2a but not for B2a and GGa1, simply because significant differences in precipitation were predicted only for A2a.

Differences in crop yields between the two downscaling methods resulted from the fundamental differences in spatial treatments of climate scenarios, and especially climate variability between the two methods. Climate scenarios and climate variability at a GCM grid box are different from those at a point scale. For simulating the site-specific impacts of climate change on crop yield, explicit spatial downscaling must be used. Results from this study clearly showed the importance of procedures or methods used for developing daily weather data for a target station under climate change for input to crop models. This finding is consistent with that reported by Mearns et al. (2003) and Tsvetsinskaya et al. (2003). They studied the effect of spatial scale of climatic change scenarios on simulated maize and winter wheat yield at various spatial scales in the Southeastern US. They directly applied relative climate changes, projected by a GCM at 300-km grids and a RCM at 50-km grids, to historical daily climatology at selected target stations using the conventional change factor method to generate daily weather data of changed climate. The RCM was used to dynamically downscale GCM output to finer spatial resolution. They found that the spatial scales (300-km vs. 50-km grids) had a significant impact on simulated maize yields but not on wheat yield and further concluded that spatial resolution of climate change scenarios could be an important uncertainty in climate change impact assessments.

## 4 Conclusions

Both implicit and explicit spatial downscaling methods were used in literature to generate daily weather series for a particular location using relative climate changes projected by GCMs or RCMs at their native grid scales. The implicit methods are easy to implement but fail to consider differences between climate variability at the GCM grid scale and that at the target station. Responses of natural resources to climate change, simulated using the implicit methods, tend to reflect more of a first-order regional sensitivity, and therefore are less variable due to their areal-averaged character. The explicit spatial downscaling methods,

which explicitly consider spatial differences of climate scenarios and variability, are more appropriate for assessing the site-specific impacts of climate change on natural resources, especially for those heavily influenced by local conditions such as soil erosion and crop production. As pointed out by Diaz-Nieto and Wilby (2005) in a similar study, differences in treating climate natural variability, temporal structuring of daily climate variables, and large-scale forcing of local climate variables between the change factor and sophisticated spatial downscaling methods are responsible for differences in impact assessments. Different spatial downscaling methods (spatial treatments) often lead to statistically different realizations of daily weather series and therefore to different outcomes in impact assessments. Relative climate changes downscaled with the explicit method in this study appeared more dynamic or variable than those with the implicit method, especially for precipitation. Consequently, the responses assessed with the explicit method seemed more dynamic and sensitive than those with the implicit method that tends to reflect more of a regional-aggregated trend. The contrasting results between the two methods show that spatial treatment of climate change scenarios can be a significant source of uncertainty and thus underscore the importance of proper spatial downscaling prior to impact simulation.

The explicit and implicit methods used in this study predicted a general increase in precipitation and temperature during 2010–2039 at Changwu. Compared to the baseline, percent changes in annual precipitation estimated by the implicit method were 15.6 and 2.0% greater than those estimated by the explicit method for A2a and B2a, respectively, and 4.9% less for GGa1. Annual mean temperatures estimated with the explicit method were 0.38, 0.34, and 0.17°C higher than those estimated with the implicit method for A2a, B2a, and GGa1, respectively.

The sensitivities of runoff and soil loss increases to precipitation increases were remarkably affected by the downscaling methods. For a 1% increase in precipitation, percent increases in average annual runoff (soil loss) were 3–6 (4–10) times greater with the explicit downscaling than those with the implicit downscaling under three climate change scenarios. Compared with the implicit method, the explicit method predicted less precipitation but greater soil loss for A2a and B2a. This is because the explicit method predicted greater variance of daily precipitation, which led to more and heavier storms, and thus greater soil loss. This result is further substantiated by individual soil loss events. Probability distributions of event soil loss estimated with the explicit method were more spread than those estimated with the implicit method. These results also indicate that soil loss is more sensitive than runoff to precipitation changes, especially changes in variance of daily precipitation.

Contrasting grain yields were found between the two downscaling methods. Compared with the baseline climate, the percent increases in wheat yield estimated with the implicit method were about 31% in all three climate change scenarios, while those estimated with the explicit method were – 1% in A2a, 23% in B2a, and 41% in GGa1. The percent increases in maize yield estimated with the implicit (explicit) method were approximately 45% (15) in A2a, 33% (23) in B2a, and 38% (38) in GGa1. The considerable differences in crop yields between the two downscaling methods demonstrated the importance of considering the spatial scale effects of climate change scenarios on impact assessments. For the site-specific assessments, explicit spatial downscaling is more appropriate for predicting crop yields using process-based models.

The explicit method downscales climate change scenarios from GCM grid scales to a target station by explicitly considering spatial variability using transfer functions. The technique suffers from the same shortcomings as all statistical downscaling methods, as it largely relies on the applicability of transfer functions to future climate. Transfer functions in this study are established based on distributions of observed and retrospectively projected

monthly values. Thus, so long as future monthly projections fall in the ranges within which transfer functions are derived, those functions are perfectly applicable to future climate. However, the validity is questioned if future projections are outside the ranges. To diminish outliers, the technique is better used with longer baseline records and for 'nearer-future' projections (say, next 20–30 years).

**Acknowledgements** The GCM data were supplied by the Climate Impacts LINK Project (DEFRA Contract EPG I/I/I24) on behalf of the Hadley Centre and U.K. Meteorological Office. This work was partially supported by the Outstanding Overseas Chinese Scholars Fund of Chinese Academy of Sciences (No. 2005-2-3) and a grant of National Natural Science Foundation of China (No. 40640420061). The author would also like to thank Dr. M.R. O'Neal and three anonymous reviewers for their insightful reviews and constructive comments.

## References

Chen YZ, Jing K, Cai JG (1988) Modern soil erosion and conservation on the Loess Plateau. Science, Beijing, PRC, pp 194 (in Chinese)

Diaz-Nieto J, Wilby RL (2005) A comparison of statistical downscaling and climate change factor methods: implications on low flows in the River Thames, United Kingdom. Clim Change 69:245–268

Favis-Mortlock DT, Savabi MR (1996) Shifts in rates and spatial distribution of soil erosion and deposition under climate change. In: Anderson MG, Brooks SM (eds) Advances in hillslope processes. Wiley, New York, pp 529–560

Flanagan DC, Nearing MA (eds) (1995) USDA-Water erosion prediction project: hillslope profile and watershed model documentation, NSERL report no. 10. USDA-ARS Nat. Soil Erosion Research Lab, West Lafayette, IN

Gordon C, Cooper C, Senior CA, Banks H, Gregory JM, Johns TC, Mitchell FB, Wood RA (2000) The simulation of SST, sea ice extents and ocean heat transports in a version of the Hadley Centre coupled model without flux adjustments. Clim Dynamics 16:147–168

Hansen JW, Ines AVM (2005) Stochastic disaggregation of monthly rainfall data for crop simulation studies. Agric For Meteorol 131:233–246

Hegerl GC, Zwiers FW, Stott PA, Kharin VV (2004) Detectability of anthropogenic changes in annual temperature and precipitation extremes. J Climate 17:3683–3700

Hewitson B (2003) Developing perturbations for climate change impact assessments. Transactions of American Geophysical Union. EOS 84:337–348

IPCC (Intergovernmental Panel on Climate Change) (2001) Climate change 2001: the scientific basis. Cambridge University Press, Cambridge, UK

Karl TR, Knight RW (1998) Secular trends of precipitation amount, frequency, and intensity in the United States. Bull Amer Meteor Soc 79:231–241

Katz RW (1996) Use of conditional stochastic models to generate climate change scenarios. Clim Change 32:237–255

Kilsby CG, Cowpertwait PSP, O'Connell PE, Jones PD (1998) Predicting rainfall statistics in England and Wales using atmospheric circulation variables. Int J Climatol 18:523–539

Mavromatis T, Jones PD (1998) Comparison of climate change scenario construction methodologies for impact assessment studies. Agric For Meteorol 91:51–67

Mearns LO, Rosenzweig C, Goldberg R (1997) Mean and variance change in climate scenarios: methods, agricultural applications, and measures of uncertainty. Clim Change 35:367–396

Mearns LO, Giorgi F, McDaniel L, Shields C (2003) Climate scenarios for the Southeastern U.S. based on GCM and regional model simulations. Clim Change 60:7–35

Nearing MA, Jetten V, Baffaut C, Cerdan O, Couturier A, Hernandez M, Le Bissonnais Y, Nichols MH, Nunes JP, Renschler CS, Souchere V, van Oost K (2005) Modeling response of soil erosion and runoff to changes in precipitation and cover. Catena 61:131–154

Nicks AD, Gander GA (1994) CLIGEN: A weather generator for climate inputs to water resource and other models. In: Proceedings of the 5th International Conference on Computers in Agriculture. American Society of Agricultural Engineers, St. Joseph, MI, pp 3–94

O'Neal MR, Nearing MA, Vining RC, Southworth J, Pfeifer RA (2005) Climate change impacts on soil erosion in Midwest United States with changes in crop management. Catena 61:165–184

Pope VD, Gallani ML, Rowntree PR, Stratton RA (2000) The impact of new physical parameterizations in the Hadley Centre Climate Model-HadAM3. Clim Dynamics 16:123–146

Pruski FF, Nearing MA (2002) Climate-induced changes in erosion during the 21st century for eight U.S. locations. Water Resour Res 38:1298

Savabi MR, Arnold JG, Nicks AD (1993) Impact of global climate change on hydrology and soil erosion: a modeling approach. In: Eckstein Y, Zaporozec A (eds) Proceedings of industrial and agricultural impact of environmental and climatic change on global and regional hydrology. Water Environment Federation, Alexandria, VA, pp 3–18

Semenov MA, Barrow EM (1997) Use of a stochastic weather generator in the development of climate change scenarios. Clim Change 35:397–414

Smith SJ, Thomson AM, Rosenberg NJ, Izaurralde RC, Brown RA, Wigley TL (2005) Climate change impacts for the conterminous USA: an integrated assessment. Clim Change 69:7–25

SWCS (2003) Conservation implications of climate change: Soil erosion and runoff from cropland. A report from the Soil and Water Conservation Society. Soil and Water Conservation Society, Ankeny, IA. (http://www.swcs.org/docs/climate%20change-final.pdf)

Tsvetsinskaya EA, Mearns LO, Mavromatis T, Gao W, McDaniel L, Downton MW (2003) The effect of spatial scale of climatic change scenarios on simulated maize, winter wheat, and rice production in the Southeastern United States. Clim Change 60:37–71

U.S. NAST (2001) Climate change impacts on the United States: the potential consequences of climate variability and change. Foundation Rep. U.S. Global Change Res. Program, Washington, DC

Wilby RL (1997) Non-stationarity in daily precipitation series: implications for GCM down-scaling using atmospheric circulation indices. Int J Climatol 17:439–454

Wilby RL, Wigley TML, Conway D, Jones PD, Hewitson BC, Main J, Wilks DS (1998) Statistical downscaling of general circulation model output: a comparison of methods. Water Resour Res 34:2995–3008

Wilks DS (1992) Adapting stochastic weather generation algorithms for climate change studies. Clim Change 22:67–84

Wilks DS (1999) Multisite downscaling of daily precipitation with a stochastic weather generator. Clim Res 11:125–136

Wood AW, Leung LR, Sridhar V, Lettenmaier DP (2004) Hydrologic implications of dynamical and statistical approaches to downscaling climate model outputs. Clim Change 62:189–216

Yu B (2005) Adjustment of CLIGEN parameters to generate precipitation change scenarios in southeastern Australia. Catena 61:196–209

Zhai P, Sun A, Ren F, Liu X, Gao B, Zhang Q (1999) Changes of climate extremes in China. Clim Change 42:203–218

Zhang XC (2005) Spatial downscaling of global climate model output for site-specific assessment of crop production and soil erosion. Agric For Meteorol 135:215–229

Zhang XC (2006) Spatial sensitivity of predicted soil erosion and runoff to climate change at regional scales. J Soil and Water Conserv 61:58–64

Zhang XC, Liu WZ (2005) Simulating potential response of hydrology, soil erosion, and crop productivity to climate change in Changwu tableland region on the Loess Plateau of China. Agric For Meteorol 131:127–142

Zhang XC, Nearing MA (2005) Impact of climate change on soil erosion, runoff, and wheat productivity in central Oklahoma. Catena 61:185–195

Zhang XC, Nearing MA, Garbrecht JD, Steiner JL (2004) Downscaling monthly forecasts to simulate impacts of climate change on soil erosion and wheat production. Soil Sci Soc Am J 68:1376–1385